# Regulating energy transfer of excited carriers and the case for excitation-induced hydrogen dissociation on hydrogenated graphene

Junhyeok Bang[a], Sheng Meng[b], Yi-Yang Sun[a], Damien West[a], Zhiguo Wang[c], Fei Gao[c], and S. B. Zhang[a,1]

[a]Department of Physics, Applied Physics, and Astronomy, Rensselaer Polytechnic Institute, Troy, NY 12180; [b]Laboratory for Surface Physics, Beijing National Laboratory for Condensed-Matter Physics and Institute of Physics, Chinese Academy of Sciences, Beijing 100190, China; and [c]Interfacial Chemistry and Engineering, Pacific Northwest National Laboratory, Richland, WA 99352

Edited by James R. Chelikowsky, University of Texas at Austin, Austin, TX, and accepted by the Editorial Board December 4, 2012 (received for review June 16, 2012)

**Understanding and controlling of excited carrier dynamics is of fundamental and practical importance, particularly in photochemistry and solar energy applications. However, theory of energy relaxation of excited carriers is still in its early stage. Here, using ab initio molecular dynamics (MD) coupled with time-dependent density functional theory, we show a coverage-dependent energy transfer of photoexcited carriers in hydrogenated graphene, giving rise to distinctively different ion dynamics. Graphene with sparsely populated H is difficult to dissociate due to inefficient transfer of the excitation energy into kinetic energy of the H. In contrast, H can easily desorb from fully hydrogenated graphane. The key is to bring down the H antibonding state to the conduction band minimum as the band gap increases. These results can be contrasted to those of standard ground-state MD that predict H in the sparse case should be much less stable than that in fully hydrogenated graphane. Our findings thus signify the importance of carrying out explicit electronic dynamics in excited-state simulations.**

photodissociation | nonadiabatic dynamics | first-principles calculation

Carrier dynamics are a key to the understanding of energy transfer in molecules and solids (1). Recent advances in femtosecond and attosecond laser techniques have also led to heightened interest in excited-state dynamics (2, 3). However, the theory of nonradiative energy relaxation of excited carriers is still rather immature. One of the fundamental reasons for this immaturity is the difficulty in going beyond the Born–Oppenheimer approximation (BOA) (4). The BOA allows us to simulate ground-state dynamics and determine the structure and phonon modes (5). However, inferring the behavior of excited states from ground-state dynamics is physically unfounded (6).The physical quantity to be examined during the dynamics is the system energy, which can be divided into kinetic energy (KE) and potential energy (PE) of the ions. The latter includes electron kinetic energy and electron–electron, electron–ion, and ion–ion interactions. Therefore, electron excitation always increases the PE of the ions. Because the excited state is not in equilibrium, the excited carriers must undergo relaxation. Among several possible relaxation mechanisms, the electron–electron (e-e) and electron–phonon (e-ph) coupling are the dominant processes in the femtosecond time regime whereas the timescales for others such as radiative recombination are about three to four orders of magnitude longer (7). In the case of e-e coupling, the energy exchange takes place only within the electronic degree of freedom, and the energy of the excited carriers is dissipated to background electrons without changing the overall PE of the ions. In contrast, in the case of e-ph coupling, the excited PE is transferred to the KE of the ions, and the KE of the ions is increased. Depending on the energy transfer mechanism, excited-state dynamics can show qualitatively different behaviors and therefore the energy transfer mechanism is the key to the understanding of the excited-state dynamics.

The direction of the energy transfer can be expected to strongly depend on the electronic structure of the system. For example, electrons in a metal can easily exchange energy because there is no band gap. The same is true for an electron–hole pair with excess energy, as the energy can be easily transferred to surrounding electrons. In contrast, excited carriers at the band edges of a semiconductor are not allowed to relax by e-e coupling unless the structure changes. By shutting down the e-e channel, the e-ph coupling becomes the dominant carrier relaxation mechanism.

Hydrogen on graphene is a good example to study the effect. Depending on the H coverage, the band gap of graphene changes from nearly zero at low coverage to 3.7 eV at high coverage (8, 9). Experiments have established that a laser can be used to manipulate H on graphene (10–12). Hydrogenated graphene not only represents a case of reactive adsorption of gas molecules on low-dimension structures for clean fuel storage (13–15), but also attracts considerable current interest for its potential in realizing graphene-based electronics by tuning the electronic properties of the graphene (8, 9, 16). By stripping off the H (12, 17), one can carve hydrogenated graphene into nanosize functional units seamlessly joined together by conductive Dirac fermions. One can also use optical excitation to prepare graphene from hydrogenated or oxidized graphene, known as graphene oxide.

In this paper, we show how electronic band structure manifests itself in the energy transfer of photoexcited carriers into surrounding electrons and H as kinetic energy, KE(H). We determine the condition for the transfer to go preferentially to H, causing dissociation. As it turns out, in the isolated H limit, both the channel to KE(H) (via e-ph coupling) and that to electronic energy (via e-e coupling) are open. Consistent with the large mass difference between electron and proton, the e-e channel is noticeably more effective than the e-ph channel. As such, KE(H) never gets large enough to dissociate the H. The situation changes as more H is added. Due to the band gap increase, the H-derived antibonding state eventually becomes the conduction band minimum (CBM). As such, the e-e channel for the electron is blocked. Our simulation for graphane shows that a majority of the energy transfer must now take place in displacing H, eventually causing its dissociation.

Author contributions: J.B. and S.B.Z. designed research; J.B. performed research; J.B. and S.M. contributed new reagents/analytic tools; J.B., S.M., Y.-Y.S., D.W., Z.W., and F.G. analyzed data; and J.B. and S.B.Z. wrote the paper.

The authors declare no conflict of interest.

This article is a PNAS Direct Submission. J.R.C. is a guest editor invited by the Editorial Board.

[1]To whom correspondence should be addressed. E-mail: zhangs9@rpi.edu.

This article contains supporting information online at www.pnas.org/lookup/suppl/doi:10.1073/pnas.1210313110/-/DCSupplemental.

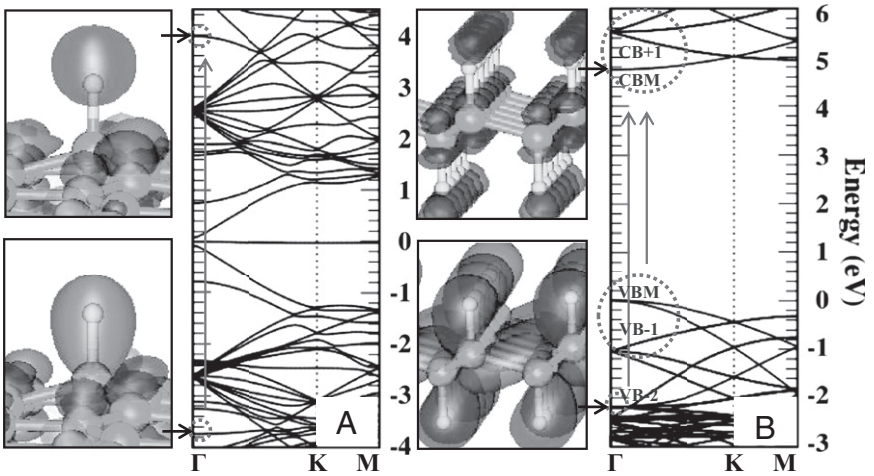


**Fig. 1.** (*A* and *B*) Band structures of isolated H on (*A*) graphene and (*B*) graphane. Vertical arrows indicate optical transitions. *Insets* show real-space charge distributions for four characteristic states.

## Results and Discussion

**Graphene with an Isolated H.** Fig. 1*A* shows the calculated band structure in which we excite one electron from the C-H bonding (BD) state to the C-H antibonding (AB) state. We focus on the time evolution of the H because energy dissipation through e-ph coupling mainly takes place here. Fig. 2*A* shows that in about 40 fs the C-H bond length is increased to 2.6 Å. However, the corresponding change in KE(H) is only about 0.1 eV. This is a strong indication that most of the energy dissipation takes place through e-e coupling. The exceptionally large C-H distance is because the electronic excitation brings the H into an excited-state potential energy surface (PES)* with a much shallower potential energy valley than the ground state, as schematically shown in Fig. 2*C*.

After the first 60 fs, H enters a period of oscillation as a result of PES evolution*, where KE(H) changes between 0 and 1.5 eV. At about 80 fs, the energy levels of both the excited electron and the hole have approached those of the Dirac point to within 0.6 eV. At this point, most of the energies of the excited carriers have dissipated. From the amplitude of the energy oscillation, we estimate that, of the 7.7-eV initial excitation, about 5.8 eV is transferred to the background electrons, and only 1.9 eV is transferred to the ions, which is not enough to dissociate H. Furthermore, due to the strong e-e coupling, even the optimal H BD to H AB excitation cannot break the C-H bond.

In the meantime, the dissipation of KE(H) into KE(C) is also significant; for example, about 0.3 eV is dissipated for $70 < t < 140$ fs. We estimate that, without a continued energy transfer from electronic excitation, most of the KE(H) will dissipate in the next 300 fs. This happens because the H stretching frequency of about 1,240 $cm^{-1}$, as determined from Fig. 2*A* (70 fs $< t <$ 140 fs), is in the range of optical phonon frequency of graphene, 1,200–1,600 $cm^{-1}$ (20).

**Fully Hydrogenated Graphane.** Fig. 1*B* shows the calculated band structure. In contrast to graphene with an isolated H, here we consider transitions across the band gap, i.e., from valence band maximum (VBM) to CBM. Because these levels are delocalized states of graphane, the contribution of a single electron–hole (e-h) pair to an individual C-H bond is negligible. The effect of excited carriers becomes significant when the excitation intensity is a fraction of the total C-H bond density.† Fig. 1*B*, *Insets* shows that the CBM and (CB +1) bands are the C-H AB states, whereas the VBM and (VB −1) bands are the delocalized C-C BD states. The (VB −2) band (which is 2 eV below the VBM) is the delocalized C-H BD states. Thermal fluctuation will break the translational symmetry of H in graphane. We mimic this effect by carrying out ground-electronic–state MD at room temperature (300 K) as input to time-dependent density functional theory: MD.

Fig. 3 shows the MD results for excitation intensity $I = 0.167$, which is defined as the ratio of the number of e-h pairs to the number of C-H bonds. At this excitation, although most of the Hs oscillate around their equilibrium positions in the 1.0- to 1.35-Å range with KE(H) < 0.35 eV/H, two of the Hs (hereby labeled as $H_{dis}$s) appear to fly away. When the C-H distance is over 1.4 Å, the corresponding KE($H_{dis}$)s exhibit a substantial linear increase, signaling the establishment of an efficient electronic energy transfer channel to the two $H_{dis}$s. Positive slopes for the two $H_{dis}$s in Fig. 3 suggest that the electronic energy transfer to KE($H_{dis}$) is initiated by a repulsive interaction of the H with surrounding atoms.

Fig. 4*A* shows the PE of the ions that oscillates around 9 eV when $t < 15$ fs. After 15 fs, however, PE decreases to 1 eV within 10 fs. Because KE without the two flying-away Hs, namely, KE(tot − 2$H_{dis}$) in Fig. 4*A*, remains largely unchanged, the electronic energy is mainly transferred to the two $H_{dis}$s, namely, KE(2$H_{dis}$). Fig. 4*B* shows the time evolutions of the occupied CBM and (CB +1) states, which oscillate due to C-H vibration. Indeed, in addition to the oscillations, these eigenvalues decrease with time. To quantify the decrease, we fitted the CBM eigenvalue by a cosine plus a linear term. The latter is shown as a dotted line in Fig. 4*B*. By contrast, there is no observable increase in the empty hole states (either VBM or VB −1) as they are carbon states of the graphane.

Note that *I* is an important parameter to the electronic energy transfer, because if the initial excitation is not sufficient to excite a significant e-ph coupling, namely, to dissociate at least one H,

*In this study, we consider the PES evolution within the framework of the quantum-classical mixed dynamics such as the Ehrenfest dynamics (6, 18). It should be noted that a more rigorous definition of the excited and time-dependent PES has recently been proposed by an exact factorization of the electron-nuclear wavefunction (19).

†In our calculation, the maximum $I = 0.25$ per C-H bond corresponds to a photoinduced electron density of about $10^{15}$ $cm^{-2}$. Hydrogen photodesorption experiments have been carried out with laser fluence in the range of 10ths or hundreds of $mJ/cm^2$ (10). A fluence of about 10 $\mu J/cm^2$ corresponds to an electron density of about $10^{12}$ $cm^{-2}$ (21). Therefore, our choices of *I* can be experimentally realized.

PHYSICS

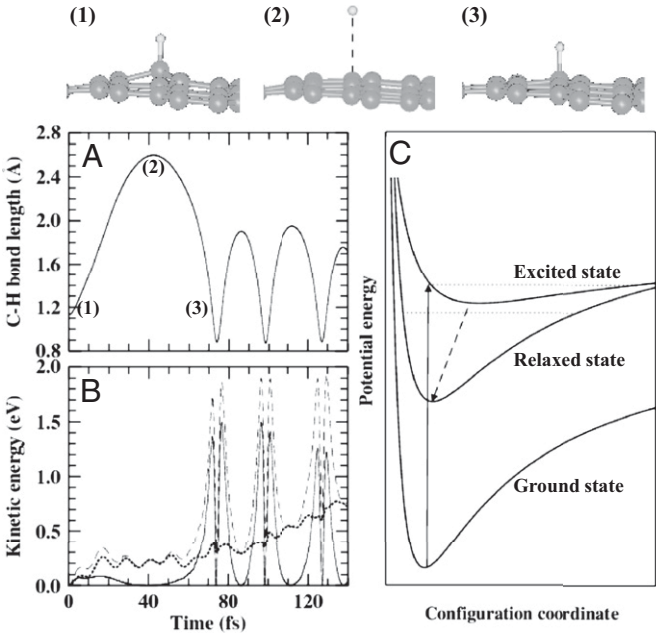


**Fig. 2.** (*A* and *B*) Time evolution of (*A*) C-H bond length and (*B*) KE for isolated H on graphene. (*C*) Schematic diagram of the PES before and after photoexcitation and its time evolution. Solid, dotted, and dashed lines in *B* stand for H, all carbon atoms, and the total system, respectively.

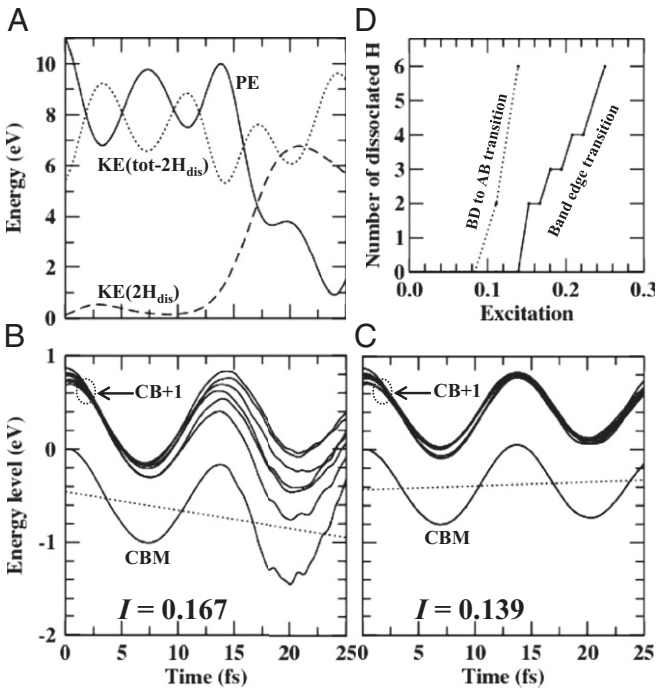


**Fig. 4.** (*A*–*C*) Time evolution of (*A*) energy and (*B* and *C*) energy levels of the CBM and (CB +1) band states with $I = 0.167$ and 0.139, respectively. In *A*, PE is rigidly shifted to 11 eV at 0 fs to show the PE in the energy scale. (*D*) Number of dissociated Hs up to $t = 25$ fs as a function of the excitation intensity.

no electronic relaxation will take place. This is illustrated in Fig. 4*C* for a smaller $I = 0.139$, where the same fit to the time evolution of the CBM state yields a slight increase, rather than a decrease.

Fig. 4*D* shows the $I$ dependences of H dissociation from which we derive the critical intensity $I_c = 0.14$ and separately the $I$ dependence for transition from the H BD state (below the VBM) to the H AB state (equal to the CBM) (Fig. 1*B*) from which we derive $I_c = 0.08$. In both cases, the blocking of the electronic relaxation at the CBM to other electronic degrees of freedom is the key for H desorption but in the latter case, the weakening of the C-H bond by the presence of excited holes further increases the likelihood of H desorption. As a result, the corresponding $I_c$ is smaller. It should be noted that $I_c$ here is only an upper bound to the actual threshold due to the relatively short simulation time: Indeed, longer simulation time for $I = 0.139$ yields one H desorption at $t = 40$ fs. To remove H from the graphane, it is desirable to use minimum $I$, because holes in the VBM or (VB −1) bands also weaken the C-C bonds, thereby giving rise to lattice rupture similar to what was calculated for ultrafast phase change materials (22).

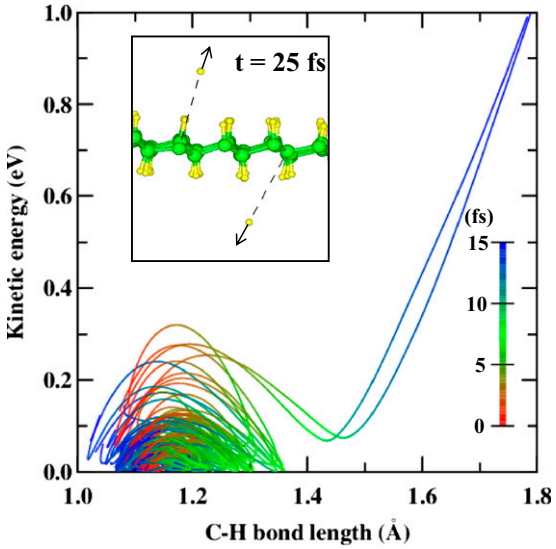


**Fig. 3.** KE with respect to C-H distance for each H in graphane with $I = 0.167$. Time evolution of the H atoms is given by the color coding. *Inset* shows the atomic structure at $t = 25$ fs.

It is known that fully H-covered graphene with $sp^3$ hybridization is more stable than graphene with low H density due to the break of the carbon π-bond network in the latter (23). However, H desorption in the former by optical excitation is easier than that in the latter. This brings us to an important question: Can photoexcitation be used to deplete H or other chemical radicals from graphene? Thermodynamically, it is known (23) that radicals want to cluster. Therefore, with thermal annealing, photoexcitation could be an effective way to remove most of the H.

## Summary

The study of H dynamics on hydrogenated graphene reveals the physics that control the energy transfer from an electronically excited state. Whereas the e-e coupling is the usual fast decaying channel, one may curb its effectiveness or completely shut down the channel by excitation to the conduction band edge. This enhances energy relaxation through the e-ph channel. In the case of a chemisorbed ligand such as hydrogen, effective photodesorption requires tuning the antibonding state to the CBM, for example, through band gap opening. It is expected that the physics here are not limited to hydrogen on graphene only. Rather, the general principle may be used to regulate photodesorption of a broad range of chemisorbed ligands on semiconductor surfaces.

## Methods

Real-time electronic and ionic dynamics calculations are carried out using ab initio MD, coupled with time-dependent density functional theory (24), as implemented in the SIESTA code (25–27). Norm-conserving Troullier–Martins pseudopotentials (28), the Perdew–Burke–Ernzerhof exchange-correlation functional (29), and the local basis set of double-$\zeta$ polarized orbitals are used. The real-space grid is equivalent to a plane-wave cutoff energy of 100 Ry. A $6 \times 6$ supercell with $\Gamma$-point sampling for the Brillouin zone integration is used. A 10-Å vacuum region is introduced between the supercells. To determine whether the vacuum region is large enough for H dissociation, we have increased it to 15 Å. The calculated H trajectories are, however, practically the same as before. Ionic coordinates are fully relaxed until the residual forces are less than 0.02 eV/Å. The electronic excitations are modeled in a phenomenological way by using constrained density functional theory calculations with the fixed occupation of the electronic states (30). We use a time step of 24 as, and the total energy is conserved to within $10^{-5}$ eV/fs per atom. A smaller time step improves the energy conservation but also significantly limits the total simulation time. At the current convergence of $10^{-5}$ eV/fs per atom, the variation of the total energy is less than 0.1 eV, which is comparable to errors from other approximations. Our simulation treats electrons quantum mechanically but treats ions classically. Such an approach is appealing because a full quantum mechanical treatment is still impractical. Within the approach, two methods have been proposed for the dynamics: the surface-hopping method (31) and the Ehrenfest method. The surface-hopping method can accurately describe trajectory bifurcation and microscopic reversibility, but has several inherent shortcomings such as unphysical discontinuities in the ionic momentum, a dependence on the choice of representation, the violation of self-consistency, and the high computational cost (6, 32). The Ehrenfest method removes these difficulties, but it may produce unphysical mixed states at the outcome. The improved Ehrenfest method solves the mixed-state problem by including a decoherence effect (33). However, implementation of the method to a large system such as ours is still intractable. For isolated H, more than 30 PESs are involved in the carrier relaxation (Fig. 1). As such, the improved Ehrenfest method is difficult to apply. Ehrenfest dynamics are the suitable approach with the assumption that decoherence time is longer than simulation time. For fully hydrogenated graphane with excitation from the valence band edge to the conduction band edge, the Ehrenfest dynamics are also valid. This is evidenced by the fact that over the simulation time of 25 fs, off-diagonal matrix elements between the conduction and valence bands are all smaller than 0.01 eV, which is small compared with the graphane band gap. Because only one PES dominates, the Ehrenfest, improved Ehrenfest, and surface-hopping dynamics are all valid approaches. Hence, we use the Ehrenfest approximation for ionic dynamics. More detailed assessment of calculation accuracy is discussed in *SI Methods: Assessment of Calculation Accuracy*.

**ACKNOWLEDGMENTS.** This work was supported by the National Nuclear Security Administration, Office of Nuclear Nonproliferation Research and Engineering, of the US Department of Energy (DOE) and by the Computational Center of Nanotechnology Innovation at Rensselaer Polytechnic Institute. F.G. and Z.W. acknowledge the use of the supercomputers in the Environmental Molecular Sciences Laboratory, a national scientific user facility sponsored by the US DOE's Office of Biological and Environmental Research. S.M. acknowledges support from National Natural Science Foundation of China (Grant 11074287) and Ministry of Science and Technology (Grant 2012CB921403).

1. Zewail AH (2000) Femtochemistry: Atomic-scale dynamics of the chemical bond. *J Phys Chem A* 104:5660–5694.
2. Corkum PB, Krausz F (2007) Attosecond science. *Nat Phys* 3:381–387.
3. Krausz F, Ivanov M (2009) Attosecond physics. *Rev Mod Phys* 81:163–234.
4. Born M, Oppenheimer JR (1927) Zur quantentheorie der molekeln [On the quantum theory of molecules]. *Ann Phys* 84:457–484.
5. Payne MC, Teter MP, Allan DC, Arias TA, Joannopoulos JD (1992) Iterative minimization techniques for ab-initio total-energy calculations - Molecular-dynamics and conjugate gradients. *Rev Mod Phys* 64:1045–1097.
6. Tully JC (1998) Mixed quantum-classical dynamics. *Farad Dicuss* 110:407–419.
7. Shah J (1991) *Ultrafast Spectroscopy of Semiconductors and Semiconductor Nanostructures*, eds Cardona M, Peter F, Klitzing K, Queisser H-J (Springer, Berlin).
8. Elias DC, et al. (2009) Control of graphene's properties by reversible hydrogenation: Evidence for graphane. *Science* 323(5914):610–613.
9. Sofo JO, Chaudhari AS, Barber GD (2007) Graphane: A two-dimensional hydrocarbon. *Phys Rev B* 75:153401.
10. Frigge R, et al. (2010) Site specificity in femtosecond laser desorption of neutral H atoms from graphite(0001). *Phys Rev Lett* 104(25):256102.
11. Siemer B, et al. (2010) Desorption of H atoms from graphite (0001) using XUV free electron laser pulses. *Chem Phys Lett* 500:291–294.
12. Wang Y, et al. (2010) Toward high throughput interconvertible graphane-to-graphene growth and patterning. *ACS Nano* 4(10):6146–6152.
13. Schlapbach L, Züttel A (2001) Hydrogen-storage materials for mobile applications. *Nature* 414(6861):353–358.
14. Dillon AC, et al. (1997) Storage of hydrogen in single-walled carbon nanotubes. *Nature* 386:377–379.
15. Patchkovskii S, et al. (2005) Graphene nanostructures as tunable storage media for molecular hydrogen. *Proc Natl Acad Sci USA* 102(30):10439–10444.
16. Bang J, Chang KJ (2010) Localization and one-parameter scaling in hydrogenated graphene. *Phys Rev B* 81:193412.
17. Sessi P, Guest JR, Bode M, Guisinger NP (2009) Patterning graphene at the nanometer scale via hydrogen desorption. *Nano Lett* 9(12):4343–4347.
18. Doltsinis NL, Marx D (2002) First principles molecular dynamics involving excited states and nonadiabatic transitions. *J Theor Comput Chem* 1:319–349.
19. Abedi A, Maitra NT, Gross EKU (2010) Exact factorization of the time-dependent electron-nuclear wave function. *Phys Rev Lett* 105:123002.
20. Maultzsch J, Reich S, Thomsen C, Requardt H, Ordejón P (2004) Phonon dispersion in graphite. *Phys Rev Lett* 92(7):075501.
21. Wang HN, et al. (2010) Ultrafast relaxation dynamics of hot optical phonons in graphene. *Appl Phys Lett* 96:081917.
22. Li XB, et al. (2011) Role of electronic excitation in the amorphization of Ge-Sb-Te alloys. *Phys Rev Lett* 107(1):015501.
23. Wang L, et al. (2010) Stability of graphene oxide phases from first-principles calculations. *Phys Rev B* 82:161406.
24. Runge E, Gross EKU (1984) Density-functional theory for time-dependent systems. *Phys Rev Lett* 52:997–1000.
25. Soler JM, et al. (2002) The SIESTA method for ab initio order-N materials simulation. *J Phys Condens Matter* 14:2745–2779.
26. Meng S, Kaxiras E (2008) Real-time, local basis-set implementation of time-dependent density functional theory for excited state dynamics simulations. *J Chem Phys* 129(5):054110.
27. Sugino O, Miyamoto Y (1999) Density-functional approach to electron dynamics: Stable simulation under a self-consistent field. *Phys Rev B* 59:2579–2586.
28. Troullier N, Martins JL (1991) Efficient pseudopotentials for plane-wave calculations. *Phys Rev B Condens Matter* 43(3):1993–2006.
29. Perdew JP, Burke K, Ernzerhof M (1996) Generalized gradient approximation made simple. *Phys Rev Lett* 77(18):3865–3868.
30. Tateyama Y, Oyama N, Ohno T, Miyamoto Y (2006) Real-time propagation time-dependent density functional theory study on the ring-opening transformation of the photoexcited crystalline benzene. *J Chem Phys* 124(12):124507.
31. Tully JC (1990) Molecular dynamics with electronic transitions. *J Chem Phys* 93:1061.
32. Hack MD, Truhlar DG (2000) Nonadiabatic trajectories at an exhibition. *J Phys Chem A* 104:7917.
33. Hack MD, Truhlar DG (2001) A natural decay of mixing algorithm for non-Born-Oppenheimer trajectories. *J Chem Phys* 114:9305.